IL NUOVO CIMENTO VOL. XXIX, N. 2 16 Luglio 1963

π^-p Interactions at 1.59 GeV/c.

SACLAY-ORSAY-BARI-BOLOGNA COLLABORATION

J. ALITTI, J. P. BATON, A. BERTHELOT, A. DAUDIN, B. DELER, O. GOUSSU, M. A. JABIOL, C. KOCHOWKI, C. LEWIN, M. NEVEU-RENÉ, A. ROGOZINSKI and F. SHIVELY

Laboratoire de Physique Corpusculaire à Haute Energie - Saclay

J. LABERRIGUE-FROLOW, NGUYEN HUU KHANH, C. OUANNÈS, M. SENÉ and L. VIGNERON

Faculté des Sciences de Paris, Laboratoire Joliot-Curie - Orsay

N. ARMENISE, S. MONGELLI, L. NITTI and A. ROMANO

Istituto di Fisica dell'Università - Bari (*)

V. ALLES-BORELLI, E. BENEDETTI, A. FORINO, G. GIACOMELLI, J. LITVAK (**), G. PUPPI, P. WALOSCHEK and W. WHITEHEAD (***)

Istituto di Fisica dell'Università - Bologna (*)
Istituto Nazionale di Fisica Nucleare - Sezione di Bologna

(ricevuto il 12 Marzo 1963)

Summary. — Report on the investigation of interactions in π^-p collisions at a pion momentum of 1.59 GeV/c, by means of the 50 cm Saclay liquid hydrogen bubble chamber, operating in a magnetic field of 17.5 kG. The results obtained concern essentially the elastic scattering and the inelastic scattering accompanied by the production of either a single pion in $\pi^-p \to p\pi^-\pi^0$ and $n\pi^-\pi^+$ interactions, or by more than one pion in four-prong events. The observed angular distribution for the elastic scattering in the diffraction region, can be approximated by an exponential law. From the extrapolated value, thus obtained for the forward scattering, one gets $\sigma_{el} = (9.65 \pm 0.30)$ mb. Effective mass spectra of $\pi^-\pi^0$

(*) This work has been supported in part by a NATO grant.

(**) From the Argentine « Comision Nacional de Energia Atomica », fellow of the « Consejo Nacional de Investigaciones Cientificas y Técnicas », of Argentina.

(***) Senior Fulbright Research Fellow.

and $\pi^-\pi^+$ dipions are given in case of one-pion production. Each of them exhibits the corresponding ρ^- or ρ^0 resonances in the region of $\sim 29\mu^2$ (μ = mass of the charged pion). The ρ peaks are particularly conspicuous for low momentum transfer (Δ^2) events. The ρ^0 distribution presents a secondary peak at $\sim 31\mu^2$ due probably to the $\omega^0 \to \pi^-\pi^+$ process. The branching ratio $(\omega^0 \to \pi^+\pi^-)/(\omega^0 \to \pi^+\pi^-\pi^0)$ is estimated to be $\sim 7\%$. The results are fairly well interpreted in the frame of the peripheral interaction according to the one-pion exchange (OPE) model, up to values of $\Delta^2/\mu^2 \sim 10$. In particular, the ratio ρ^-/ρ^0 is of the order of 0.5, as predicted by this model. Furthermore, the distribution of the Treiman-Yang angle is compatible with an isotropic one inside the ρ peak. The distribution of $\sigma_{\pi^+\pi^-}$, as calculated by the use of the Chew-Low formula assumed to be valid in the physical region of Δ^2, gives a maximum which is appreciably lower than the value of $12\pi\lambda^2 = 120$ mb expected for a resonant elastic $\pi\pi$ scattering in a $J=1$ state at the peak of the ρ. However, a correcting factor to the Chew-Low formula, introduced by SELLERI, gives a fairly good agreement with the expected value. Another distribution, namely the Δ^2 distribution, at least for $\Delta^2 < 10\,\mu^2$, agrees quite well with the peripheral character of the interaction involving the ρ resonance. π^- angular distributions in the rest frame of the ρ exhibit a different behaviour for the ρ^- and for the ρ^0. Whereas the first one is symmetrical, as was already reported in a previous paper, the latter shows a clear forward π^- asymmetry. The main features of the four-prong results are: 1) the occurrence of the $\frac{3}{2}\frac{3}{2}$ $(p\pi^+)$ isobar in $\pi^-p \to p\pi^+\pi^-\pi^-$ events and 2) the possible production of the $\omega^0 \to \pi^+\pi^-\pi^0$ resonance in $\pi^-p \to p\pi^-\pi^+\pi^-\pi^0$ events. No ρ's were observed in four-prong events.

1. – Introduction.

We present in this paper results obtained from the study of 1.59 GeV/c π^- interactions in a liquid hydrogen bubble chamber. The reactions which have been particularly considered are the following (*):

(1)	$\pi^- + p \to \pi^- + p$	(elastic scattering)
(2)	$\pi^- + \pi^0 + p$	(one-pion creation)
(3)	$\pi^- + \pi^+ + n$	(one-pion creation)
(4)	$\pi^- + \pi^- + \pi^+ + p$	(two-pion creation)
(5)	$\pi^- + \pi^- + \pi^+ + \pi^0 + p$	(three-pion creation)
(6)	$\pi^- + \pi^- + \pi^+ + \pi^+ + n$	(three-pion creation)

(*) A distinct report on strange-particle production will be published later.

Similar interactions have been investigated by many other authors [1,2].

Part of our results have already been published [1f,2a]. In [2a] we gave an analysis of events of type (2) in which the recoil proton stopped in the chamber, ensuring that only small momentum transfers were considered. By the use of the peripheral model we deduced the $\pi^-\pi^0$ scattering cross-section and by studying the angular distribution of $\pi^-\pi^0$ scattering we were led to demonstrate the resonant behaviour of the two-pion system in the $J=1$ state (the so-called ρ resonance).

In [1f] we studied the elastic diffraction scattering for small momentum transfers.

Since then the work has been extended to events involving larger momentum transfers. In addition, consideration was given to other types of reactions. The present paper is a report on this work.

---

(1) Elastic scattering: *a*) C. C. TING, L. W. JONES and M. L. PERL: *Phys. Rev. Lett.*, **9**, 468 (1962); *b*) C. LOVELACE: *Nuovo Cimento*, **25**, 730 (1962); *c*) R. BARLOUTAUD, C. CHOQUET-LOUEDEC, A. DEREM, J. HEUGHEBAERT, A. LEVEQUE and J. MEYER: *Phys. Lett.*, **1**, 207 (1962); *d*) J. A. HELLAND, T. J. DEVLIN, D. E. HAGGE, M. J. LONGO B. J. MOYER and C. D. WOOD: *Phys. Rev. Lett.*, **10**, 27 (1963); *e*) J. W. CRONIN: *Phys. Rev.*, **118**, 824 (1960); *f*) SACLAY-ORSAY-BARI-BOLOGNA COLLABORATION: *Nuovo Cimento*, **22**, 1310 (1961). Further references can be found in these papers. A review article on the subject is given by V. S. BARASHENKOV: *Fortschr. d. Phys.*, **10**, 205 (1962).

(2) Inelastic scattering with one and multipion production: *a*) D. STONEHILL, C. BALTAY, H. COURANT, W. FICKINGER, E. C. FOWLER, H. KRAYBILL, J. SANDWEISS. J. SANFORD and H. TAFT: *Phys. Rev. Lett.*, **6**, 624 (1961); *b*) A. R. ERWIN, R. MARCH, W. D. WALKER and E. WEST: *Phys. Rev. Lett.*, **6**, 628 (1961); *c*) E. PICKUP, D. K. ROBINSON and E. O. SALANT: *Phys. Rev. Lett.*, **7**, 192 (1962); *d*) SACLAY-ORSAY-BARI-BOLOGNA COLLABORATION: *Nuovo Cimento*, **25**, 365 (1962); *e*) R. BARLOUTAUD, J. HEUGHEBAERT, A. LEVEQUE, J. MEYER and R. OMNÈS: *Phys. Rev. Lett.*, **8**, 32 (1962); *f*) D. D. CARMONY and R. T. VAN DE WALLE: *Phys. Rev. Lett.*, **8**, 73 (1962); *g*) L. B. AUERBACH, T. ELIOFF, W. B. JOHNSON, J. LACH, C. E. WIEGAND and T. YPSILANTIS: *Phys. Rev. Lett.*, **9**, 173 (1962); *h*) W. SELOVE, V. HAGOPIAN, H. BRODY, A. BAKER and E. LEBOY: *Phys. Rev. Lett.*, **9**, 272 (1962); *i*) V. P. KENNEY, W. D. SHEPHARD and C. D. GALL: *Phys. Rev.*, **126**, 736 (1962); *j*) W. D. SHEPHARD and W. D. WALKER: *Phys. Rev.*, **126**, 278 (1962); *k*) I. I. SHALAMOV and A. F. GRASHIN: *Žurn. Èksp. Teor, Fiz.*, **43**, 726 (1962); *l*) D. O. CALDWELL, E. BLEULER, B. ELSNER, L. W. JONES and B. ZACHAROV: *Phys. Lett.*, **2**, 253 (1962); *m*) J. J. VEILLET, J. HENNESSY, H. BINGHAM, M. BLOCH, D. DRIJARD, A. LAGARRIGUE, P. MITTNER, A. ROUSSET, G. BELLINI, M. DI CORATO, E. FIORINI and P. NEGRI: *Phys. Rev. Lett.*, **10**, 29 (1963); *n*) C. ALFF, D. BERLEY, D. COLLEY, N. GELFAND, U. NAUENBERG, D. MILLER, J. SCHULTZ, J. STEINBERGER, T. H. TAN, H. BRUGGER, P. KRAMER and R. PLANO: *Phys. Rev. Lett.*, **9**, 322, 325 (1962); *p*) N. P. SAMIOS, A. H. BACHMAN, R. M. LEA, T. E. KALOGEROPOULOS and W. D. SHEPHARD: *Phys. Rev. Lett.*, **9**, 139 (1962); *q*) N. N. BISWAS, I. DERADO, K. GOTTSTEIN, V. P. KENNEY, D. LÜERS, G. LÜTJENS and N. SCHMITZ: *Phys. Lett.*, **3**, 11 (1962).

2. – Experimental procedure.

Figure 1 shows the beam layout. The internal proton beam of the Saclay 3 GeV proton synchrotron (Saturne) strikes a copper target placed in one of the quadrants. The π^- beam produced at 0° is deflected by 27° 20′ by the magnetic field of the accelerator; an additional momentum analysis is

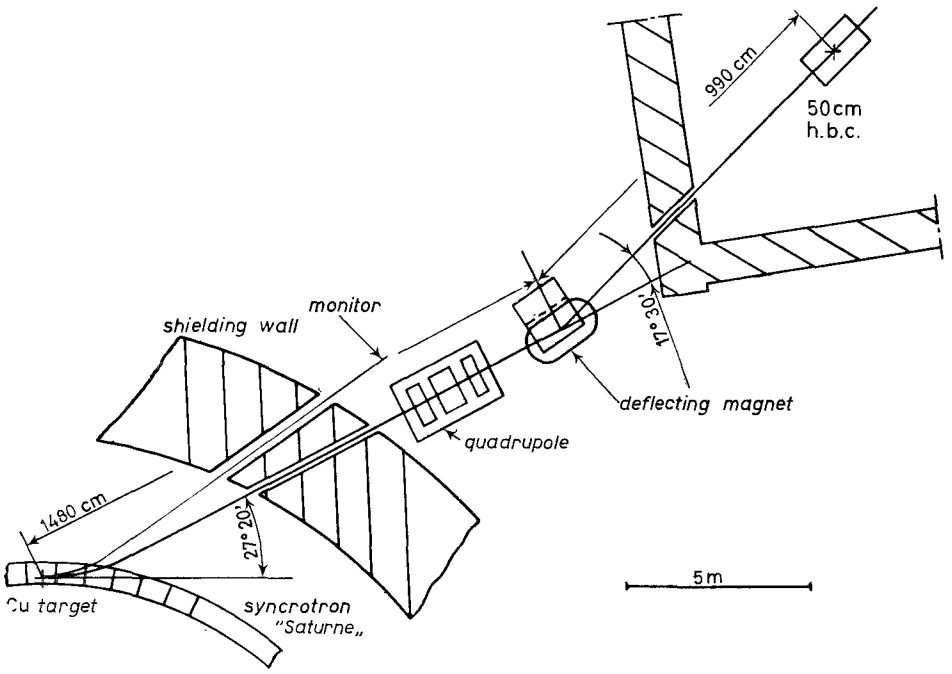

Fig. 1. – Layout of the π^- beam of 1.59 GeV/c.

performed by a magnet which deflects the beam by 17° 30′. A system of 3 quadrupole lenses of 15 cm diameter aperture, placed before the deflecting magnet, focuses the beam in the middle of the bubble chamber.

Two collimators define the required geometrical configuration of the beam. The momentum of the beam, as determined by floating wire measurements, is (1.590 ± 0.025) GeV/c. These values were confirmed:

1) by the kinematic analysis of Σ^-K^+ production events;

2) by direct curvature measurements of beam tracks.

The contamination, measured with a gas Čerenkov counter, was found to consist of $(8 \pm 2)\%$ μ^- and of less than 1% electrons. The liquid hydrogen Saclay bubble chamber of 50 cm diameter and 35 cm depth was used with a magnetic field of 17.5 kG.

About 140 000 stereoscopic pictures have been analysed. Only those events originating in a fiducial region of the chamber and having a minimum measurable track length of 15 cm for the primary particle and of 25 cm for the secondaries of two-prong events, and of 15 cm for four-prong events, were selected.

Best fits of the events were made using kinematical programs (GAP or GUTS) on IBM 7090 and 704 computers; ionization of the positive particles was systematically taken into account. A useful piece of information was always the missing mass of the event. Use of these procedures left a negligible percentage of events unclassified.

The scanning efficiency was taken into account in determining the cross-sections. It depends, of course, on the type of events considered. It was determined by rescanning part of the film; the lowest value occurred for « stops »: (81 ± 5) %. For events with charged secondaries, rescanning ensured an efficiency close to 100 %.

Table I gives a summary of the number of events of reactions (1) to (6), as well as the corresponding cross-sections.

The total cross-section of (32.5 ± 0.6) mb obtained is in good agreement with the value of (32.1 ± 1.5) mb given by BRISSON *et al.* [3].

TABLE I. – *Summary of interactions investigated and of the corresponding cross-sections.*

Type of events	Reaction	Number of events	Cross-section (mb)
Stops	Only neutral secondaries, excepted strange particles	—	4.92 ± 0.33
Two-prong events	π^-p	1704	9.65 ± 0.30
	$\pi^-\pi^0p$	934	4.48 ± 0.15
	$\pi^-\pi^+n$	1394	6.45 ± 0.17
	$p\pi^-k\pi^0$ $(k>1)$	170	0.80 ± 0.06
	$n\pi^-\pi^+k\pi^0$ $(k\geqslant 1)$	845	3.96 ± 0.14
Four-prong events	$p\pi^-\pi^-\pi^+$	570	0.88 ± 0.04
	$p\pi^-\pi^-\pi^+\pi^0$	118	0.18 ± 0.02
	$n\pi^-\pi^-\pi^+\pi^+$	74	0.12 ± 0.02
Strange particles	—	—	0.93 ± 0.10
Unclassified events	—	25	
Total cross-section	—	—	32.5 ± 0.6

The number of events reported in column 3 corresponds to total track lengths which vary from 6 to $20 \cdot 10^6$ cm according to the type of events.

3. – Elastic scattering.

Elastic events were separated from inelastic ones on the basis of coplanarity, of angular correlation, as well as of momentum-angle correlation. A best fit program was also used.

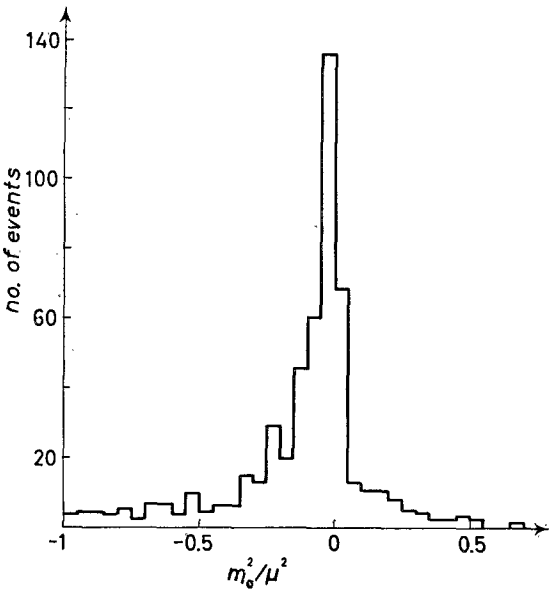

Fig. 2. – Distribution of the squared missing mass for a sample of elastic events (505 events).

Figure 2 shows the squared neutral effective mass associated with elastic events. The peak of the distribution is not exactly centered at zero mass, but at about $-0.02\,\mu^2$ (μ = = rest mass of the charged pion). It can be seen that in the selected sample of elastic events there is no appreciable contamination from inelastic events corresponding to a neutral mass of one or several π^0's.

Figure 3 gives the differential cross-section in the diffraction region as a function of the square of the four-momentum transfer Δ^2/μ^2. The experimental values are reproduced in Table II. The first six points on the low momentum transfer side, for which the proton stops in the chamber, have been previously published ([1f]).

The elastic cross-section, which cannot be measured without bias for pion laboratory scattering angles smaller than 5°, corresponding to a proton recoil range smaller than 1 cm, was determined by extrapolating the Δ^2 distribution curve. The value thus found was $\sigma_{el} = (9.66 \pm 0.30)$ mb.

As Δ^2/μ^2 and θ_{cm} are linearly related by

$$\text{(I)} \qquad \frac{\Delta^2}{\mu^2} = \frac{2p_{cm}^2}{\mu^2}(1 - \cos\theta_{cm}),$$

one finds immediately the following relation:

$$\text{(II)} \qquad \frac{d\sigma}{d(\Delta^2/\mu^2)} = \frac{\pi\mu^2}{p_{cm}^2}\left(\frac{d\sigma}{d\Omega}\right)_{cm},$$

([3]) J. C. Brisson, J. F. Detoeuf, P. Falk-Vairant, L. Van Rossum and G. Valladas: *Nuovo Cimento*, **19**, 210 (1961).

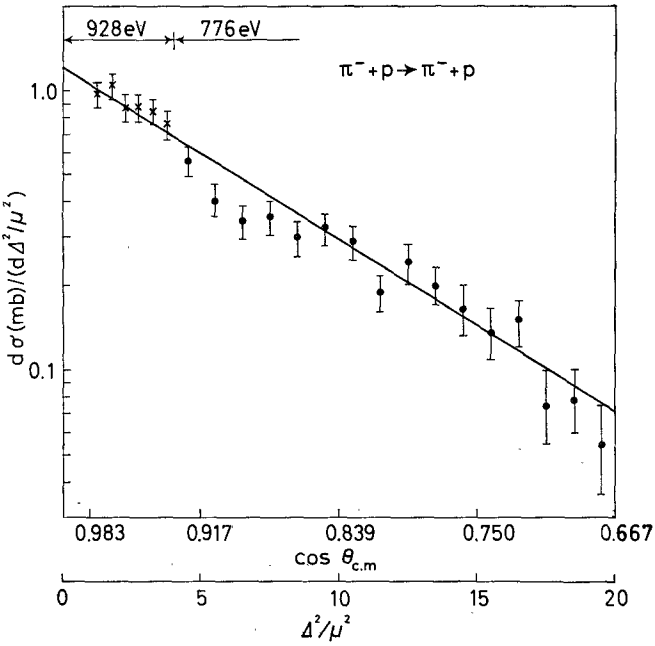

Fig. 3. – Elastic scattering differential cross-section in the diffraction region, as a function of the square of the four-momentum transfer to the nucleon. The straight line is a least squares fit of the experimental points:

$$\log \frac{d\sigma}{d\Delta^2/\mu^2} = (0.17 \pm 0.05) - (0.143 \pm 0.007)\, \Delta^2/\mu^2 .$$

where θ_{cm} and p_{cm} are, respectively, the center-of-mass scattering angle and momentum of the scattered pion.

TABLE II. – *Experimental values of the elastic scattering differential cross-section in the diffraction region.*

Δ^2/μ^2	$d\sigma$ (mb)/d(Δ^2/μ^2)	Δ^2/μ^2	$d\sigma$ (mb)/d(Δ^2/μ^2)
1.25	0.99 ± 0.09	9.5	0.318 ± 0.040
1.75	1.06 ± 0.09	10.5	0.284 ± 0.037
2.25	0.87 ± 0.08	11.5	0.189 ± 0.031
2.75	0.88 ± 0.08	12.5	0.244 ± 0.035
3.25	0.84 ± 0.08	13.5	0.204 ± 0.032
3.75	0.77 ± 0.08	14.5	0.164 ± 0.029
4.5	0.558 ± 0.053	15.5	0.139 ± 0.026
5.5	0.403 ± 0.045	16.5	0.149 ± 0.027
6.5	0.344 ± 0.042	17.5	0.074 ± 0.019
7.5	0.358 ± 0.043	18.5	0.079 ± 0.020
8.5	0.298 ± 0.039	19.5	0.054 ± 0.016

Δ^2/μ^2 is the square of the four-momentum transfer in units of μ^2, the square of the charged pion rest mass.

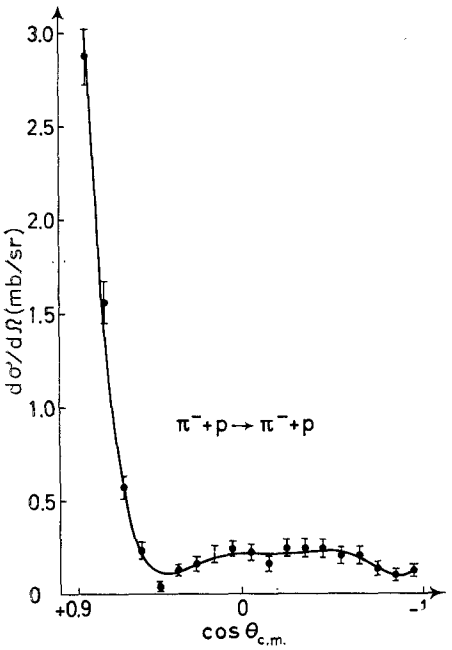

Fig. 4. – Elastic scattering differential cross-section, as a function of $\cos\theta_{cm}$.

Figure 4 shows the differential cross-section for $\cos\theta_{cm} \leqslant 0.9$. The experimental values are shown in Table III.

The large-angle cross-section (Fig. 4) shows a broad backward bump. Quite similar results have been obtained by several authors [1].

A $\sum_{k=0}^{n} a_k \cos^k\theta_{cm}$ polynomial least squares fit of the angular distribution gives, for $n=6$, the values of the coefficients a_k up to a_6 shown in Table IV. Higher order polynomials give stationary values of χ^2/ν (Fig. 5), where ν represents the number of degrees of freedom.

Simple models for diffraction scattering, such as scattering by an imaginary gaussian potential, give the following approximate expression for the differential cross-section at low momentum

TABLE III. – *Experimental values of the elastic scattering differential cross-section in the center-of-mass system.*

$\cos\theta_{cm}$	$(d\sigma/d\Omega)_{cm}$ (mb/sr)	$\cos\theta_{cm}$	$(d\sigma/d\Omega)_{cm}$ (mb/sr)
0.85	2.87 ± 0.15	— 0.05	0.22 ± 0.04
0.75	1.56 ± 0.11	— 0.15	0.16 ± 0.04
0.65	0.51 ± 0.06	— 0.25	0.25 ± 0.04
0.55	0.24 ± 0.04	— 0.35	0.25 ± 0.04
0.45	0.05 ± 0.02	— 0.45	0.25 ± 0.04
0.35	0.13 ± 0.03	— 0.55	0.21 ± 0.04
0.25	0.16 ± 0.04	— 0.65	0.21 ± 0.04
0.15	0.21 ± 0.04	— 0.75	0.14 ± 0.03
0.05	0.25 ± 0.04	— 0.85	0.10 ± 0.03
—	—	— 0.95	0.13 ± 0.03

TABLE IV. – *Coefficients of a least squares* $\sum_{k=0}^{6} a_k \cos^k\theta_{cm}$ *polynomial fit.*

a_0	a_1	a_2	a_3	a_4	a_5	a_6
0.22 ± 0.02	— 0.06 ± 0.09	— 0.60 ± 0.30	— 1.64 ± 0.53	— 0.47 ± 1.0	— 5.66 ± 0.69	4.05 ± 0.97

transfer which indicates an exponential decrease with increasing Δ^2/μ^2:

$$\text{(III)} \qquad \frac{\mathrm{d}\sigma}{\mathrm{d}(\Delta^2/\mu^2)} = \left(\frac{\mathrm{d}\sigma}{\mathrm{d}(\Delta^2/\mu^2)}\right)_0 \exp\left[-A\Delta^2/\mu^2\right],$$

where A gives the order of magnitude of the squared range of the potential, expressed in units of $\lambda\!\!\!^{-}_c$, the pion Compton wave length.

The experimental results (Fig. 3) are compatible with (III). A least squares fit calculation, represented by the straight line, gives

$$\left(\frac{\mathrm{d}\sigma}{\mathrm{d}(\Delta^2/\mu^2)}\right)_0 = (1.18 \pm 0.06)\ \text{mb}, \quad \text{per unit of } \Delta^2/\mu^2.$$

$$A = (0.14 \pm 0.01).$$

However, it can be seen from Fig. 3 that the exponential fit should be considered as a first approximation and that a possible existence of some kind of structure inside the diffraction peak cannot be excluded.

From (II) and (III) one obtains, as $p_{\mathrm{cm}} = 0.75$ GeV/c,

$$\left(\frac{\mathrm{d}\sigma}{\mathrm{d}\Omega}\right)_0 = \frac{p_{\mathrm{cm}}^2}{\pi\mu^2}\left(\frac{\mathrm{d}\sigma}{\mathrm{d}(\Delta^2/\mu^2)}\right)_0 = (10.9 \pm 0.6)\ \text{mb/sr}.$$

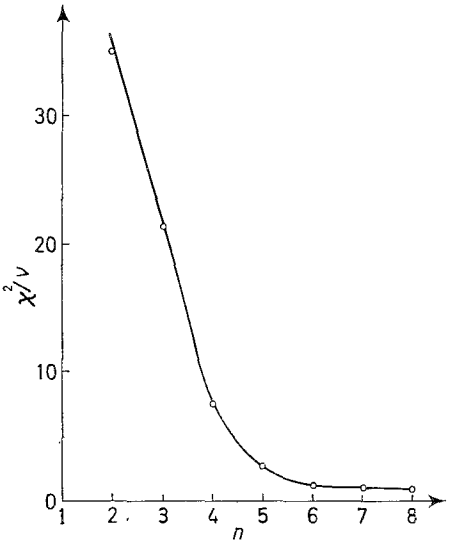

Fig. 5. – χ^2/ν distribution, as a function of the degree n of a least squares $\sum_{k=0}^{n} a_k \cos^k\theta_{\mathrm{cm}}$ polynomial fit applied to the angular distribution of Fig. 4; ν represents the number of degrees of freedom.

Comparing this value with the square of the imaginary part of the forward scattering amplitude obtained from the optical theorem with $\sigma_{\mathrm{total}} = 32.1\,\mathrm{mb}$ [3](*), where

$$\mathrm{Im}\, f(0) = \frac{k}{4\pi}\sigma_{\mathrm{total}} = 0.975 \cdot 10^{-13}\ \mathrm{cm},$$

one can estimate the real part of the forward scattering amplitude:

$$|\mathrm{Re}\, f(0)|^2 = \left(\frac{\mathrm{d}\sigma}{\mathrm{d}\Omega}\right)_0 - |\mathrm{Im}\, f(0)|^2 = (1.4 \pm 0.6)\ \text{mb/sr}.$$

(*) *Note added in proof.* – More recent results [A. N. DIDDENS, E. W. JENKINS, T. F. KYCIA and K. F. RILEY: *Phys. Rev. Lett.*, **10**, 262 (1963)] indicate a value of $\sigma_{\mathrm{total}} \simeq 34$ mb, which would lead to $|\mathrm{Re}\, f(0)|^2$ compatible with zero.

The value of $|\mathrm{Re}\, f(0)|^2$ is thus of the order of 15 % of $|\mathrm{Im}\, f(0)|^2$, within the limits of errors. This result is in agreement with the value of $\mathrm{Re}\, f(0)$ given by CRONIN ([16]) for the same energy.

4. – One-pion creation.

4·1. *Mass spectra of two-particle systems.* – For the events of reactions (2) and (3) the effective mass ω of the dipion systems $(\pi^-\pi^0)$ and $(\pi^-\pi^+)$ has been determined. Figure 6 shows the two mass spectra as a function of ω^2/μ^2. The relativistically invariant phase-space spectrum has also been plotted for the sake of comparison.

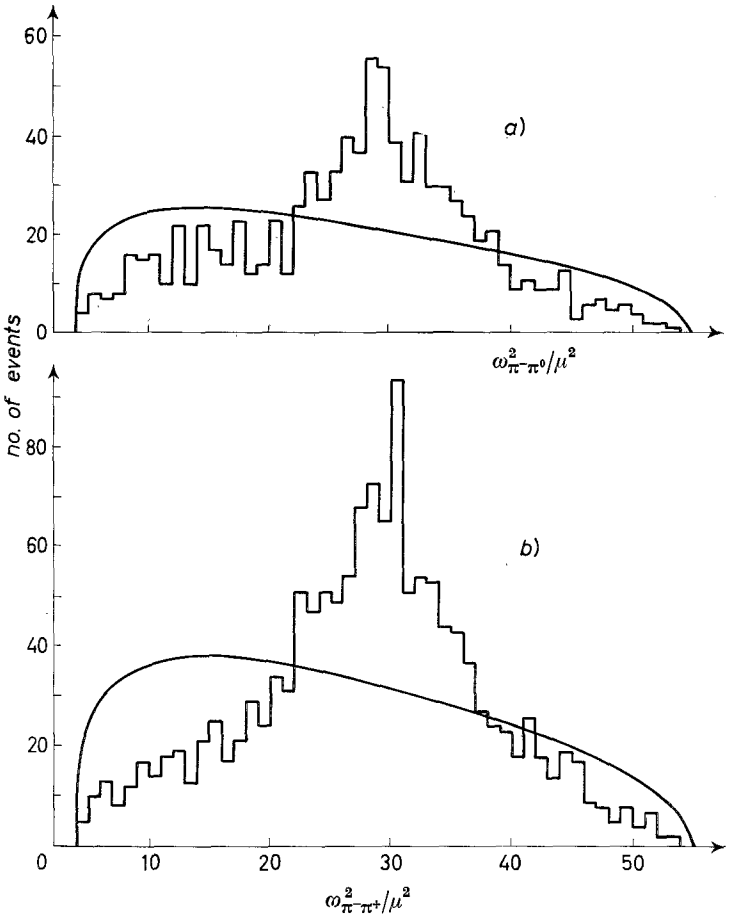

Fig. 6. – $(\pi^-\pi^0)$ and $(\pi^+\pi^-)$ mass spectra; solid curves represent invariant phase-space distributions normalized to the corresponding number of events: *a*) total $\pi^-\pi^0$ mass spectrum, 932 events; *b*) total $\pi^+\pi^-$ mass spectrum, 1394 events.

Both distributions show a well-pronounced peak at $\omega^2 = 29\,\mu^2$ corresponding to the ρ. With the possible exception of a small spike around $\omega^2 = 31\,\mu^2$ in the $(\pi^-\pi^+)$ spectrum, no significant difference appears between the two spectra, suggesting the dominant role of the ρ in pion production in this mass region.

DALITZ plots have been made for both reactions. By projecting these on the appropriate axes one obtains the mass spectra for pion-nucleon systems, $(p\pi^-)$, $(p\pi^0)$, $(n\pi^+)$ and $(n\pi^-)$ (Fig. 7). The general aspect of these spectra is

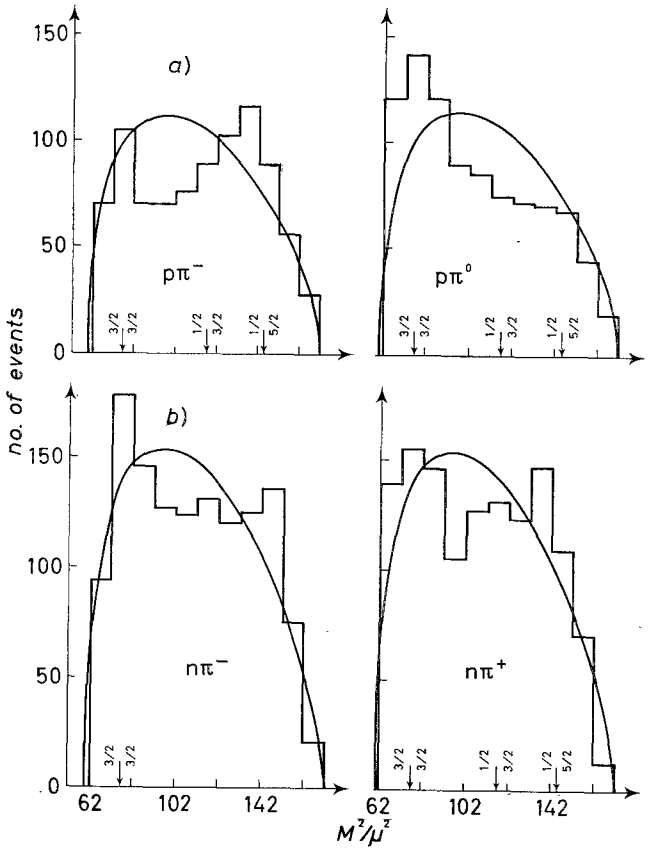

Fig. 7. – $(p\pi^-)$, $(p\pi^0)$, $(n\pi^-)$ and $(n\pi^+)$ mass spectra; solid curves represent invariant phase-space distributions normalized to the corresponding number of events: *a*) $\pi^-p \to \pi^-\pi^0p$; *b*) $\pi^-p \to \pi^+\pi^-n$.

quite different from the one which should be observed if the processes were dominated by the pion-nucleon interaction and more precisely by the $\frac{3}{2}\frac{3}{2}$ isobar.

We thus conclude that the final state interaction between two-pions is the most important feature of the processes considered. However, to obtain a more precise description we analysed their behaviour as a function of Δ^2/μ^2.

4·2. *Mass spectrum of the dipions for different intervals of the four-momentum transfer.* – Figure 8 shows the dipion mass spectra for four different intervals of Δ^2/μ^2.

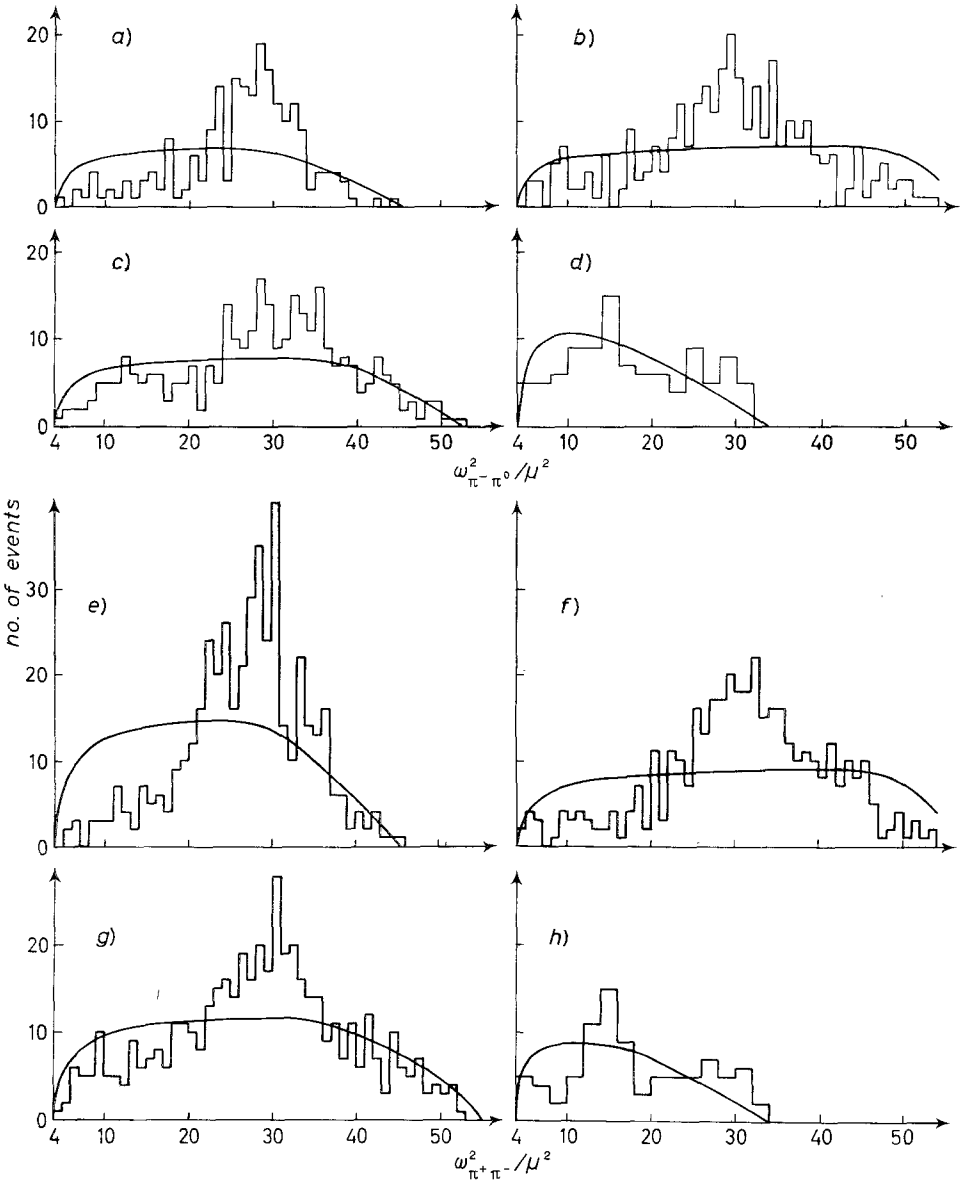

Fig. 8. – $(\pi^-\pi^0)$ and $(\pi^+\pi^-)$ mass spectra for different intervals of Δ^2/μ^2; solid curves represent invariant phase-space distributions normalized to the corresponding number of events: $\pi^-p \to \pi^-\pi^0 p$: *a*) $1.5 \leqslant \Delta^2/\mu^2 < 8$, 211 events; *b*) $8 \leqslant \Delta^2/\mu^2 < 25.5$, 308 events; *c*) $25.5 \leqslant \Delta^2/\mu^2 < 73$, 313 events; *d*) $\Delta^2/\mu^2 \geqslant 73$, 102 events; $\pi^-p \to \pi^+\pi^- n$: *e*) $1.5 \leqslant \Delta^2/\mu^2 < 8$, 447 events; *f*) $8 \leqslant \Delta^2/\mu^2 < 25.5$, 393 events; *g*) $25.5 \leqslant \Delta^2/\mu^2 < 73$, 463 events; *h*) $\Delta^2/\mu^2 \geqslant 73$, 90 events.

Three remarks can be made:

a) The ρ peak, which is more apparent in the low momentum transfer events, has completely disappeared for the highest values of Δ^2/μ^2.

b) For events with $\Delta^2/\mu^2 > 73$ one sees a small peak at $\omega^2 \sim 16\,\mu^2$, both in the $\pi^-\pi^0$ and in the $\pi^-\pi^+$ spectra. Adding those two spectra (Fig. 9), the peak emerges from phase-space by ~ 2 standard deviations. However, due to poor statistics, we are not able to ascertain that this peak is not accidental. Nevertheless, it is worth-while to mention its occurrence, since it appears at the same value of ω^2 in the neutral and negative dipion spectra, and since peaks have already been reported in the same energy region, *e.g.* [4].

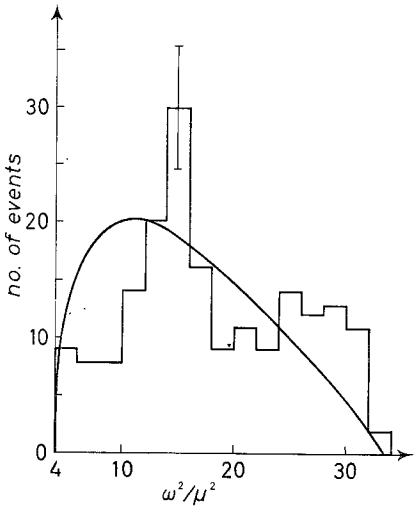

Fig. 9. – Combined $(\pi^-\pi^0)$ and $(\pi^-\pi^+)$ mass spectrum for $\Delta^2/\mu^2 \geqslant 73$ (192 events).

c) The peak in the $(\pi^+\pi^-)$ spectrum at about 31 μ^2 remains apparent up to $\Delta^2/\mu^2 = 73$. It is tempting to relate this peak, at least partly, to the $\pi^+\pi^-$-decay of ω^0. The possibility of occurrence of such an effect in experimental data has already been considered by several authors [2n,5-7].

Figure 10 shows the difference between the total spectra of $(\pi^+\pi^-)$ and of $(\pi^-\pi^0)$ normalized to the same number of events. From this one can roughly estimate the contribution of ω^0 to be something like 30 events (~ 0.14 mb). In order to deduce from this value the branching ratio for the $\pi^+\pi^-$ decay of ω^0, we need the number of ω^0 events produced through the process

$$\pi^- + \mathrm{p} \to \omega^0 + \mathrm{n}\,.$$

---

[4] B. Sechi Zorn: *Phys. Rev. Lett.*, **8**, 282 (1962).

[5] W. D. Walker, E. West, A. R. Erwin and R. H. March: *Intern. Conf. on High-Energy Physics at CERN* (1962), p. 42.

[6] T. Toohig, R. Kraemer, L. Madansky, M. Meer, M. Nussbaum, A. Pevsner C. Richardson, R. Strand and M. Block: *Intern. Conf. on High-Energy Physics at CERN* (1962), p. 99.

[7] J. B. Shafer, J. J. Murray, D. O. Huwe, F. Solmitz and M. L. Stevenson: *Bull. Am. Phys. Soc.*, **8**, 22 (1963).

An estimate of the branching ratio of this process can be made in the following way: assuming that all $(n\pi^+\pi^- k\pi^0)$ events, the cross-section of

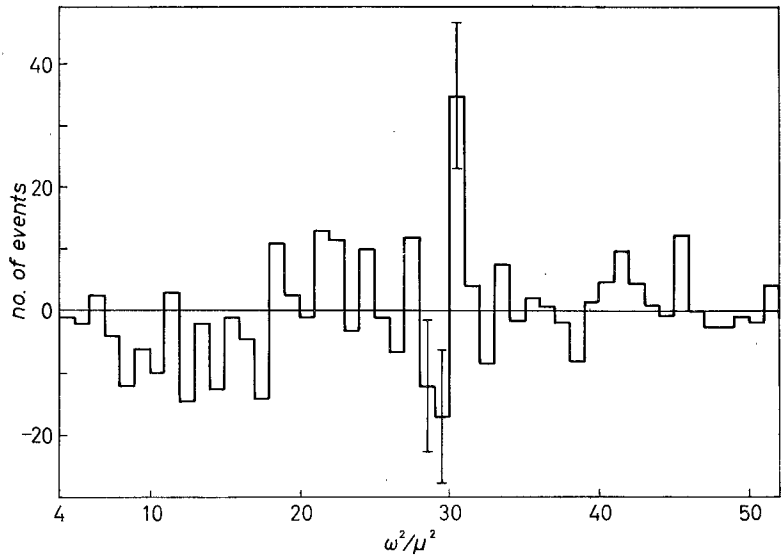

Fig. 10. – Difference between $(\pi^-\pi^-)$ and $(\pi^-\pi^0)$ total mass spectra, where the $(\pi^-\pi^0)$ spectrum was normalized by a factor b to the $(\pi^-\pi^+)$ spectrum.

which is ~ 4 mb according to Table I, correspond to the above reaction, a lower limit of the branching ratio is

$$r = \frac{\omega^0 \to 2\pi}{\omega^0 \to 3\pi} \simeq \frac{0.14}{4} \approx 3.5\,\% .$$

Actually, not all $(n\pi^+\pi^- k\pi^0)$ events are ω^0 events. According to the data of WALKER *et al.* [5] and of TOOHIG *et al.* [6], a reasonable value for the production cross-section of $\omega^0 \to 3\pi$ would be ~ 2 mb for the present energy: hence $r \simeq 7\,\%$. J. STEINBERGER *et al.* [2n] find $r \leqslant 2\,\%$.

4·3. *Contribution of the* $\frac{3}{2}\,\frac{3}{2}$ *isobar.* – The effective masses of the three two-particle compounds $(\pi^+\pi^-)$, $(n\pi^-)$ and $(n\pi^+)$ which can be considered in the final state of the $\pi^- p \to n\pi^+\pi^-$ interaction are connected by the following relation:

$$M^2_{\pi^+\pi^-} + M^2_{n\pi^-} + M^2_{n\pi^+} = W^2 + M^2_n + 2\mu^2 ,$$

where W is the total energy available in the overall $\pi^- p$ c.m.; in the present case $W = 1.970$ GeV. A Dalitz plot can be made with these variables.

Owing to the peculiar, strongly forward peaked angular distribution of the scattered π^- in the ρ^0 rest system (cf. Fig. 21), the Dalitz plot exhibits, on pure kinematical grounds, a concentration of events at one extremity of the ρ band (instead at the two extremities as was the case for the ρ^-, the angular distribution of which was peaked forward and backward, cf. Fig. 7 in ([2d])).

When projected on the $n\pi^-$ and $n\pi^+$ axes, this concentration, which is particularly important at low Δ^2 values, due to the peripheral formation of ρ, gives rise to the maxima which can be observed at the higher extremity of the $M^2_{(n\pi^-)}$ and at the lower extremity of the M^2 spectra (Fig. 11). It is particularly worth noticing that there is no significant peaking which could be attributed to the $\frac{3}{2}\,\frac{3}{2}$ $n\pi^-$ isobar. This confirms the interpretation already given in ([2d]).

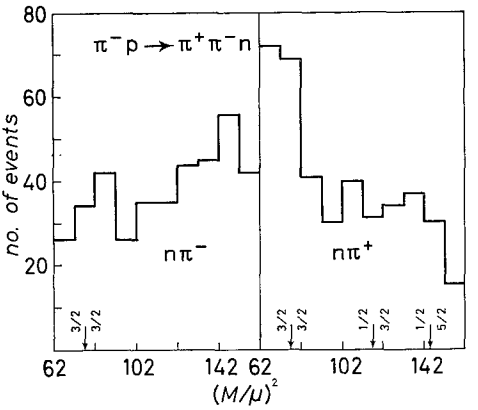

Fig. 11. – $(n\pi^-)$ and $(n\pi^-)$ mass spectra for $1.5 \leqslant \Delta^2/\mu^2 < 8$.

However when one looks at the mass spectra of the π-$\mathcal{N}$ systems for larger Δ^2-values, for which the ρ formation is less important, it can be seen that a small contribution of the $\frac{3}{2}\,\frac{3}{2}$ isobar cannot be excluded (Fig. 7*a* and 7*b*).

4·4. *The one-pion exchange model.* – The distribution of events (Fig. 12) as a function of Δ^2/μ^2 shows a strong accumulation in the region of small Δ^2/μ^2, as already pointed out in many previous papers ([2]).

This state of affairs which is called « peripheral » production can be reasonably understood on the basis of a model, in which the preference for small momentum transfers results from the emission by the nucleon of a virtual pion which scatters on the incident one (the so-called OPE mechanism).

Typical peripherism is achieved when it is possible to isolate the contribution of the pole at $\Delta^2/\mu^2 = -1$ from other contributions, a part of which one generally represents by some kind of form factor. Thus, the dependence of the differential cross-section $d\sigma/d(\Delta^2/\mu^2)$ on Δ^2/μ^2 may be written

$$\frac{d\sigma}{d(\Delta^2/\mu^2)} = \frac{\Delta^2/\mu^2}{[(\Delta^2/\mu^2)+1]^2} H(\Delta^2/\mu^2) .$$

The characteristic feature of the peripheral interaction arises essentially from the $\Delta^2/(\Delta^2+\mu^2)^2$ term which gives a strong peak at $\Delta^2 = \mu^2$. The function $H(\Delta^2/\mu^2)$ produces a displacement of the peak toward a higher value of Δ^2;

the main part of the Δ^2 distribution remains nevertheless concentrated around low values of Δ^2, as can be seen from the theoretical curve of Fig. 19.

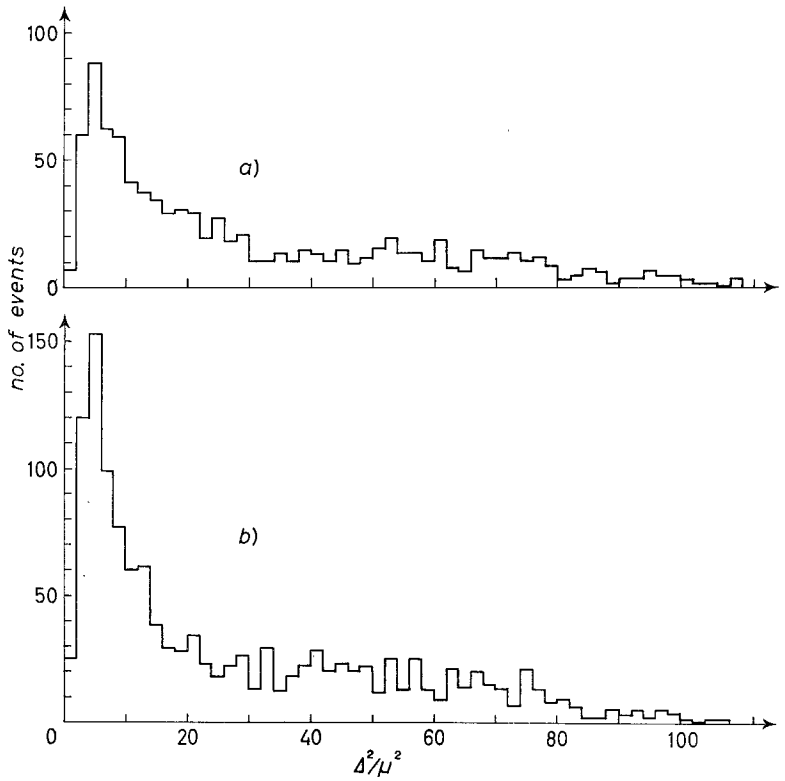

Fig. 12. – Distribution of Δ^2/μ^2, the squared four-momentum transfer to the nucleon: *a*) $\pi^-p \to \pi^-\pi^0 p$; *b*) $\pi^-p \to \pi^-\pi^+ n$.

Several tests of the validity of the peripheral hypothesis have been proposed and some consequences have been deduced of its supposed correctness.

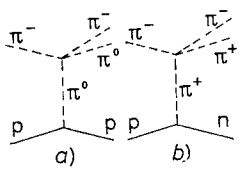

Fig. 13. – Feynman graphs for the one-pion exchange processes.

a) $p\pi^-\pi^0/n\pi^+\pi^-$ ratio. This ratio is the product of two Clebsch-Gordan coefficients coming from the two upper vertices of graphs *a*) and *b*) (Fig. 13). If one assumes that the interaction at the pion-pion vertex is in a pure $T=1$ state, it is easily found that the ratio $p\pi^-\pi^0/n\pi^+\pi^-$ should be $\frac{1}{2}$. The experimental result for $\Delta^2/\mu^2 < 8$ is (0.47 ± 0.06) when all values of ω are considered and (0.59 ± 0.09) when they are restricted to the ρ region $(25 \leqslant \omega^2/\mu^2 \leqslant 33)$. These values are in good agreement with the expected value of $\frac{1}{2}$.

If one considers the same ratio for larger values of Δ^2/μ^2, it is seen from

Fig. 14 that substantial deviations from $\frac{1}{2}$ occur, indicating that the OPE model is no longer valid.

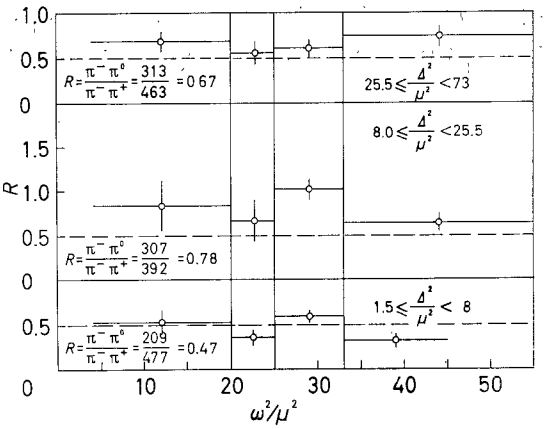

Fig. 14. – Ratio of reactions (2) and (3), as a function of Δ^2/μ^2.

b) The Treiman-Yang test. TREIMAN and YANG [8] have proposed a test of the validity of the OPE model. Since the particle which propagates between the two vertices of graphs *a*) and *b*) (Fig. 13) is spinless, the angular distributions involved at these two vertices should be independent. The situation is best visualized in a frame of reference in which the incoming pion is at rest.

In this frame (Fig. 15), the lines of flight of the incident and the final nucleons define a plane Π_i, while the two final pions define a plane Π_f which intersect along the line of flight of the virtual exchanged pion. The OPE model implies that the angle α_{TY} between the two planes should be uniformly distributed. Fig. 16 *a*) and *b*) show, for $1.5\leqslant\Delta^2/\mu^2<8$, the distributions of α_{TY} for events of type (2) and (3), in the ρ-region ($25\leqslant\omega^2/\mu^2\leqslant33$) and outside the ρ-region. It is seen that the first ones, for both signs of the dipion, are in good agreement with a uniform distribution. Indeed, a χ^2 test for a uniform distribution gives a value of 12 inside the ρ^- and ρ^0 peaks and of 24 outside: these values give respectively ~0.85 and ~0.15 for the corresponding probabilities. Attention should be called to the fact that isotropy still holds up to the highest values of Δ^2/μ^2 inside the ρ peak (Fig. 16 *c*), *e*)). On the contrary, outside the ρ peak, a certain trend toward anisotropy can be observed (Fig. 16 *d*), *f*)).

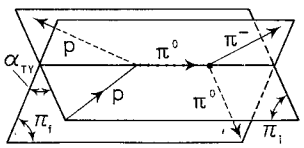

Fig. 15. – Production and decay planes (Π_i and Π_f) of the dipion in the « antilaboratory » system in which the incoming pion is at rest. α_{TY} is the Treiman-Yang angle.

Another test is to look for a possible dependence of the angular distribution in the π-π scattering on the angle α_{TY}. The OPE model ensures that no such dependence should exist. Figure 17 shows the angular distributions for $\pi^-\pi^+$ events and for mall values of Δ^2/μ^2, with $0<\alpha_{TY}<90°$ or $90°<$

---

[8] S. B. TREIMAN and C. N. YANG: *Phys. Rev. Lett.*, **8**, 140 (1962).

$< \alpha_{TY} < 180°$. No difference between the two distributions can significantly be noticed; on the other hand, the asymmetry parameter is the same within the limits of error for both distributions.

This result disagrees with that of PICKUP *et al.* [9], who worked however with a π^- beam of lower energy.

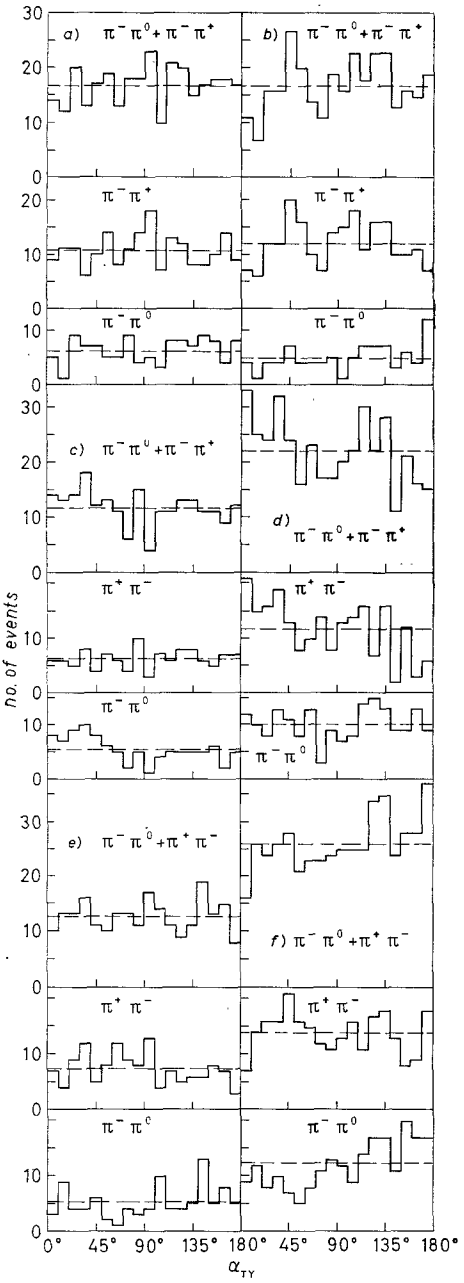

Fig. 16. – Distribution of the Treiman-Yang angle α_{TY} for the indicated dipion events for different Δ^2/μ^2 values. Dashed lines represent isotropic distributions normalized to the corresponding number of events: *a*), *c*), *e*) inside the ρ peak; *b*), *d*), *f*) outside.

a) $1.5 \leqslant \Delta^2/\mu^2 < 8$, $25 \leqslant \omega^2/\mu^2 \leqslant 33$;

b) $1.5 \leqslant \Delta^2/\mu^2 < 8$, $\omega^2/\mu^2 < 25$, $\omega^2/\mu^2 > 33$;

c) $8 \leqslant \Delta^2/\mu^2 < 25.5$, $25 \leqslant \omega^2/\mu^2 \leqslant 33$;

d) $8 \leqslant \Delta^2/\mu^2 < 25.5$, $\omega^2/\mu^2 < 25$, $\omega^2/\mu^2 > 33$;

e) $25.5 \leqslant \Delta^2/\mu^2 < 73$, $25 \leqslant \omega^2/\mu^2 \leqslant 33$;

f) $25.5 \leqslant \Delta^2/\mu^2 < 73$, $\omega^2/\mu^2 < 25$, $\omega^2/\mu^2 > 33$.

(9) E. PICKUP, D. K. ROBINSON and E. O. SALANT: *Phys. Rev. Lett.*, **9**, 170, 242 (E) (1962).

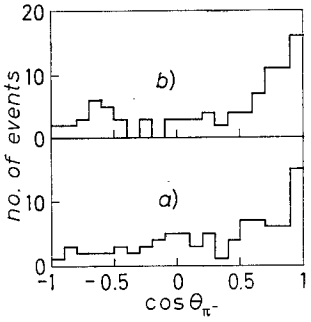

Fig. 17. – Angular distributions, for $\pi^-p \to \pi^-\pi^+n$ interactions, of the scattered π^- with respect to the incoming π^-, both considered in the rest frame of the dipion, for events:

a) with $0° \leqslant \alpha_{TY} \leqslant 90°$;
$7 \pm 0.10 = 32/86 = 0.3(F-B)/(F+B)$;

b) with $90° < \alpha_{TY} \leqslant 180°$;
$(F-B)/(F+B) = 38/92 = 0.41 \pm 0.10$.

These distributions refer to events with low Δ^2/μ^2 values and inside the ρ peak: $1.5 \leqslant \Delta^2/\mu^2 < 8$, $25 \leqslant \omega^2/\mu^2 \leqslant 33$.

c) The $\sigma_{\pi\pi}$ cross-section. The question of the $\pi\pi$ cross-section and of the resonant nature of the state $T=1$, $J=1$ has been discussed for $\pi^-p \to \to \pi^-\pi^0p$ low momentum transfer events in a previous paper ([2d]). It was pointed out there that the cross-section calculated using the Chew-Low ([10]) formula in the physical region of small Δ^2/μ^2 ($\leqslant 4$) was appreciably lower

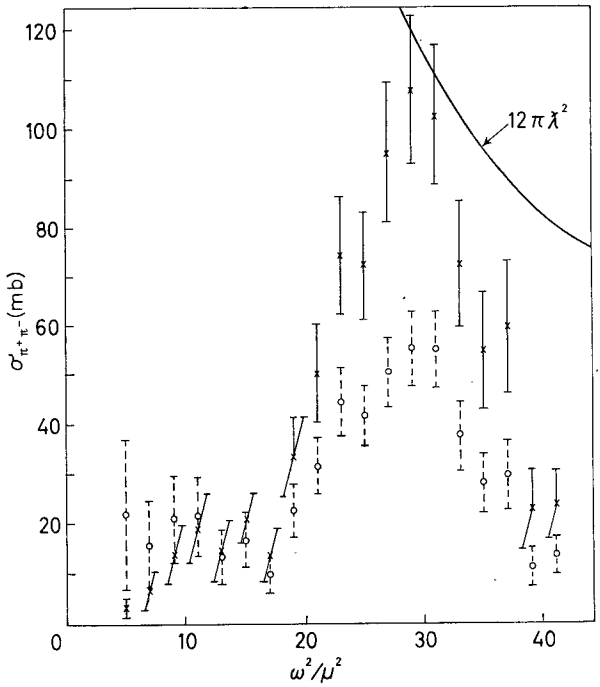

Fig. 18. – $(\pi^-\pi^+)$ cross-section, as a function of the squared mass of the dipion for small momentum transfers ($1.5 \leqslant \Delta^2/\mu^2 < 8$); solid line represents the cross-section for resonant scattering in a $J=1$ state: o Chew-Low formula; × Selleri formula.

([10]) G. F. CHEW and F. E. LOW: *Phys. Rev.*, **113**, 1640 (1959).

than the expected value of $12\,\pi\lambda\!\!\!^{-2} = 120$ mb at the resonance, for a pure $J=1$ state.

Since then the results were completed for $\pi^- p \to \pi^- \pi^+ n$ events with $\Delta^2/\mu^2 < 8$ (Fig. 18). In this case $\sigma_{\pi^+\pi^-}$ reaches a maximum value of (56 ± 8) mb, which is again appreciably lower than $12\,\pi\lambda\!\!\!^{-2}$.

A reasonable interpretation of this discrepancy has been proposed by SELLERI [11] in terms of a factor F related to the pionic form factor of the nucleon. The main point of this proposal consists in using the same function F to explain the one-pion production in processes (2) and (3), on the one hand, and the one-pion production in nucleon-nucleon interactions, on the other hand.

According to this procedure, the Chew-Low formula should be replaced by

$$\text{(IV)} \qquad \begin{cases} \dfrac{\mathrm{d}^2\sigma}{\mathrm{d}(\Delta^2/\mu^2)\,\mathrm{d}(\omega^2/\mu^2)} = \left[\dfrac{p}{q} F(\Delta^2/\mu^2)\right]^2 \left[\dfrac{\mathrm{d}^2\sigma}{\mathrm{d}(\Delta^2/\mu^2)\,\mathrm{d}(\omega^2/\mu^2)}\right]_{\text{Ch. L.}}, \\ F(\Delta^2/\mu^2) = \dfrac{0.72}{1 + \dfrac{(\Delta^2/\mu^2)+1}{4.73}} + 0.28\,, \end{cases}$$

where p and q are respectively the momenta of the incident and of the scattered π^-, both expressed in the dipion rest system.

The maximum value of $\sigma_{\pi^+\pi^-}$ obtained is (108 ± 16) mb, in fairly good agreement with the expected value of $12\,\pi\lambda\!\!\!^{-2}$.

d) The momentum transfer spectrum. The experimental Δ^2 spectrum is given in Fig. 19, for $20 \leqslant \omega^2/\mu^2 \leqslant 38$, centered around the ρ peak. The solid curve has been calculated by the Chew-Low formula, as modified by the above Selleri term; one thus obtains

$$(5) \qquad \frac{\mathrm{d}\sigma}{\mathrm{d}(\Delta^2/\mu^2)} = \frac{f^2\mu^2}{2\pi q_{iL}^2} \frac{\Delta^2/\mu^2}{[(\Delta^2/\mu^2)+1]^2} \left(F \frac{p_r}{q_r}\right)^2 \int_{(\omega/\mu)^2_{\min}}^{(\omega/\mu)^2_{\max}} \frac{\omega}{\mu} \sqrt{\frac{\omega^2}{4\mu^2} - 1}\, \sigma_{\pi\pi}(\omega)\, \mathrm{d}\frac{\omega^2}{\mu^2},$$

where the lower and the upper limits of the integral are given by the Chew-Low [10] phase-space curve, correlating ω^2/μ^2 to Δ^2/μ^2 and where p_r and q_r are the respective values of p and q at the resonance.

Both theoretical curves, obtained without any normalization, give the right position of the maximum of the distributions.

It should be recalled that the validity of formula (IV) probably extends only up to $\Delta^2/\mu^2 \simeq 10$.

---

[11] F. SELLERI: *Phys. Lett.*, **3**, 76 (1962).

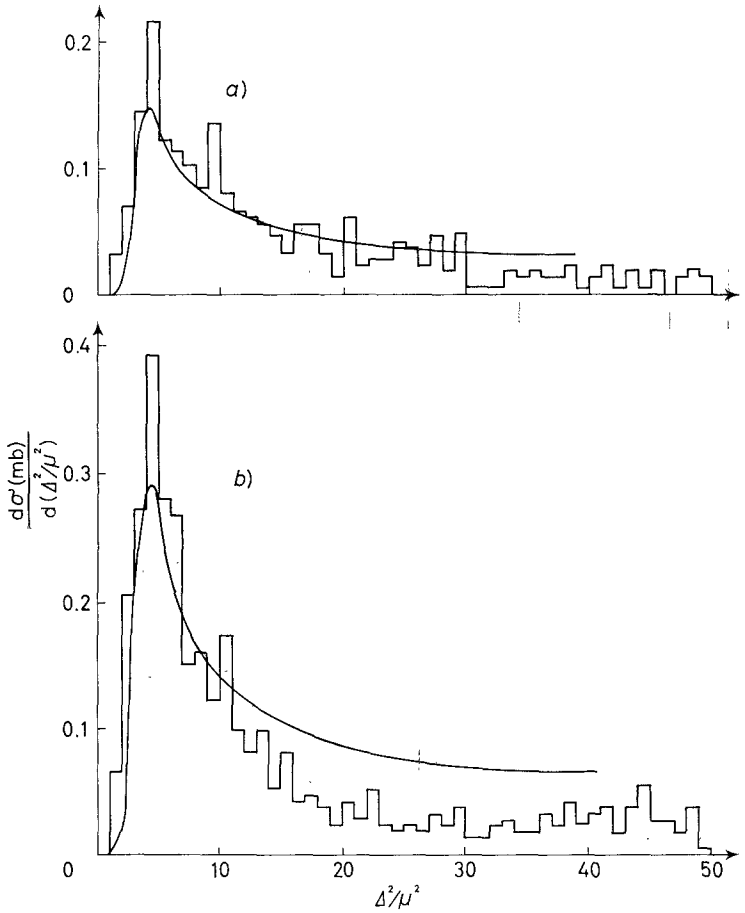

Fig. 19. – Δ^2/μ^2 distributions for events centered around the ρ peak ($20 \leqslant \omega^2/\mu^2 \leqslant 38$). The solid lines represent the theoretical distributions according to the formula of Chew and Low as modified by SELLERI: *a*) $\pi^-p \to \pi^-\pi^0 p$; *b*) $\pi^-p \to \pi^-\pi^+ n$.

e) The π-π scattering angular distribution. Assuming the validity of the OPE model, one can interpret the angular distribution of the two-pions existing in the final state as the result of the scattering of the real pion (the incident one) on a virtual pion of squared mass equal to $-\Delta^2$ (formula (1.16) in ([10])). It may be expected that for small Δ^2/μ^2 this angular distribution will not be significantly different from that obtained in the scattering of two real pions.

As suggested by CHEW and LOW, the correct procedure would be to extrapolate the angular distribution obtained as a function of Δ^2/μ^2, to $\Delta^2/\mu^2 = -1$. Unfortunately, this requires a statistical accuracy which is not available in

the present data. Therefore we have to use at face value the results corresponding to small Δ^2/μ^2 events.

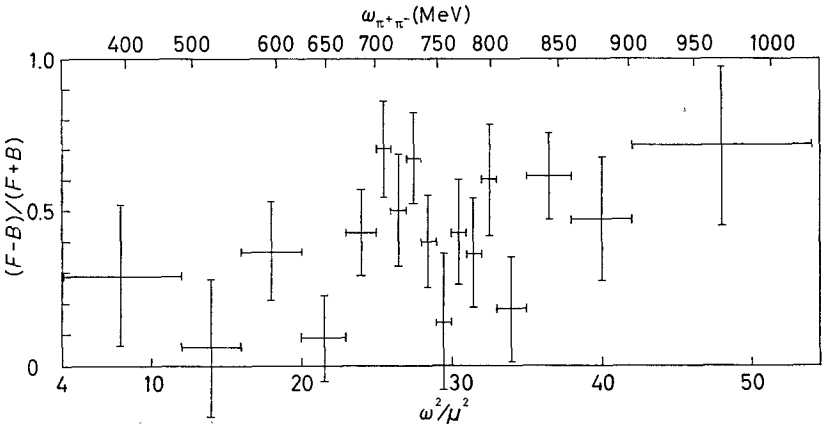

Fig. 20. – Asymmetry parameter, as a function of the mass of the $(\pi^-\pi^+)$ dipion for low momentum transfers ($1.5 \leqslant \Delta^2/\mu^2 < 8$).

Little information can be added to what has been reported in the previous paper ([2d]) concerning $\pi^-\pi^0$ scattering. Let us recall only that the dominant feature of the obtained results has been the particular shape of the asymmetry parameter A= (Forward — Backward)/(Forward+Backward), which goes through zero for an effective mass of the dipion corresponding closely to the peak of the ρ.

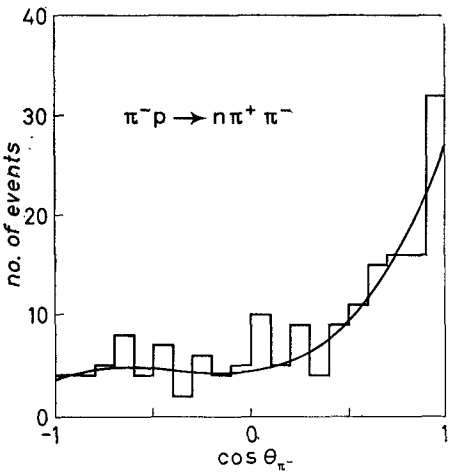

Fig. 21. – Angular distribution of the scattered π^- with respect to the incoming π^-, both considered in the rest frame of the dipion. This distribution refers to events with small momentum transfer and inside the ρ peak: ($25 \leqslant \omega^2/\mu^2 \leqslant 33$, $1.5 \leqslant \Delta^2/\mu^2 < 8$). The solid curve represents a best fit polynomial of third degree in cos θ_{π^-}.

Results for $\pi^-\pi^+$ are quite different, as A changes sign nowhere and remains positive for the whole range of ω^2/μ^2. Figure 20 is a plot of the asymmetry parameter as a function of ω^2/μ^2. Its general behaviour is that of a slowly rising function with an interfering term in the ρ region. This interference appears to be positive between $\omega^2 = 25\,\mu^2$ and $29\,\mu^2$ and negative between $29\,\mu^2$ and $31\,\mu^2$. There seems to be at present no unambiguous interpretation of such a result.

If one tries to fit the differential cross-section in the ρ region with a cos θ

polynomial, it is found that no good fit can be obtained unless one uses at least a third-degree polynomial (Fig. 21). In the hypothesis that the OPE model describes the situation this would imply the occurrence of a D-wave in a $T=0$ state, since nothing of this kind was found for $\pi^-\pi^0$.

5. – Four-prong events.

The events giving rise to nucleon-pion four-prong patterns may be classified in the following reactions:

(4) $\pi^-\mathrm{p} \to \mathrm{p}\,\pi^-\pi^-\pi^+$

(5) $\mathrm{p}\,\pi^-\pi^-\pi^+\pi^0$

(6) $\mathrm{n}\,\pi^-\pi^-\pi^+\pi^+$

(7) $\mathrm{p}\,\pi^-\pi^-\pi^+(k\pi^0)$ $\quad k\geqslant 2$

(8) $\mathrm{n}\,\pi^-\pi^-\pi^+\pi^+(k\pi^0)$ $\quad k\geqslant 1$

In reactions (7) and (8), because at least two neutral particles are produced, only partial kinematical analysis is possible and our study has been concentrated on the three first reactions.

5·1. $\mathrm{p}\pi^-\pi^-\pi^+$ *events.* – 570 events have been identified in this group, corresponding to a production cross-section of (0.88 ± 0.04) mb. The « effective mass » of any possible combination of two and three particles has been calculated and the corresponding « effective mass » spectra have been plotted and compared to relativistically invariant phase-space prediction.

The most significant deviation from phase-space may be observed for $(\mathrm{p}\pi^+)$ events. Figure 22 shows the experimental mass spectrum together with the phase-space spectrum normalized to the same number of events. It is clearly seen that there is an excess of events around 1210 MeV and this can be ascribed to the formation of the $\frac{3}{2}\,\frac{3}{2}$ $(\mathrm{p}\pi^+)$ isobar.

The deviations from phase space which are observed in the other « effective mass » spectra may be interpreted as consequences of the enhancement of the $(\mathrm{p}\pi^+)$ isobar formation.

A typical case is that of the $(\mathrm{p}\pi^-\pi^-)$ mass spectrum which is shown in Fig. 23. Comparison with the phase-space spectrum may lead one to conclude that something looking like an isobar is formed around 1700 MeV. It is easy to see that the peak appearing at this energy is the reflection of the one appearing in the $(\mathrm{p}\pi^+)$ mass spectrum. Figure 24 shows the curve inside of which

the experimental points must lie in a $(p\pi^+)(p\pi^-\pi^-)$ plot, as imposed by energy and momentum conservation; points which lie around 1210 MeV on the $(p\pi^+)$ axis, must lie around 1700 MeV on the $(p\pi^-\pi^-)$ axis.

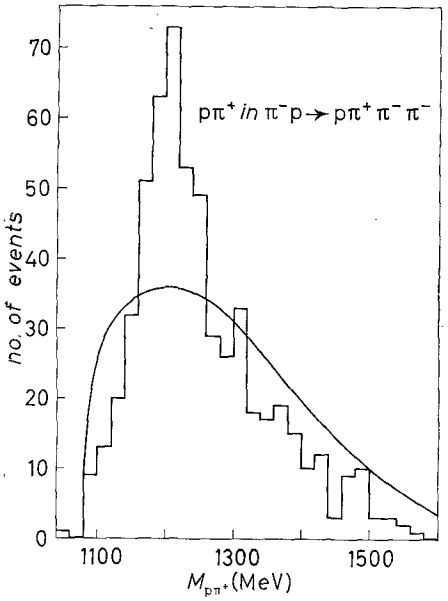

Fig. 22. – $(p\pi^+)$ mass spectrum (570 events).

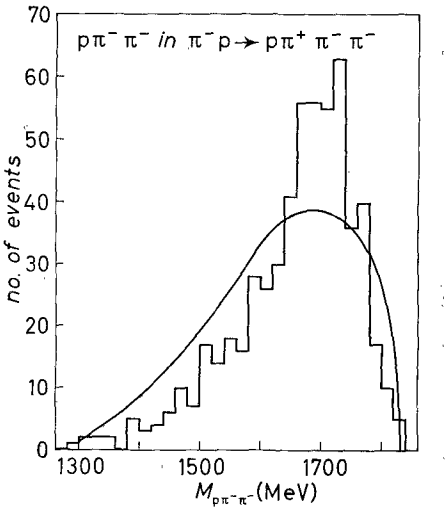

Fig. 23. – $(p\pi^-\pi^-)$ mass spectrum (570 events).

Another illustration is given by the distortion of the $(\pi^-\pi^-)$ mass spectrum. Figure 25 *a*) and 25 *b*) show respectively the mass spectra for events in which the associated $(p\pi^+)$ mass is inside or outside the isobar region (1160 MeV $< M_{p\pi^+} <$ < 1280 MeV). It appears clearly that, while the second one is consistent with the statistical distribution, the first one is somewhat distorted in favour of higher $(\pi^-\pi^-)$ masses.

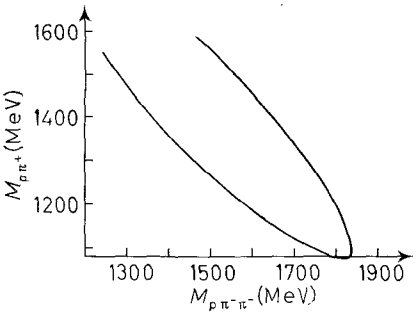

Fig. 24. – Kinematical limits, as imposed by energy-momentum conservation for a $(p\pi^+)$, $(p\pi^-\pi^-)$ plot.

What is the mechanism which could explain the favoured production of the $(p\pi^+)$ isobar? One of the frequently proposed models is the OPE model giving rise to long-range or peripheral interaction, as represented by the diagram of Fig. 26 *a*). The extreme opposite would be to include all possible kinds of short-range interactions, as symbolized by the « bubble » of Fig. 26 *b*) and to interpret the isobar production as due to final-state interaction between the proton and the π^+.

As the shape of the mass spectrum does not seem to be a sufficiently sensitive test to choose between the models, we have looked for a more specific criterium. In particular, one may expect that, if the diagram of Fig. 26 *a*) is dominant, the squared momentum-transfer to the isobar has a spectrum of the ChewLow type, *i.e.*, with a strong maximum for very small Δ^2. This is not the case, as shown by Fig. 27, where this spectrum is plotted separately for events for which the $(p\pi^+)$ mass lies inside (Fig. 27 *a*)) and outside (Fig. 27 *b*)) the isobar region. Moreover, the two spectra look alike within the limits of statistical accuracy, as can be seen from Fig. 27 *d*) which shows the ratio of the two spectra as a function of Δ^2.

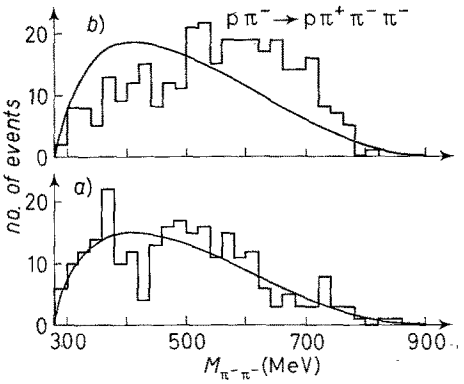

Fig. 25. – $(\pi^-\pi^-)$ mass spectra: *a*) events for which the associated $(p\pi^+)$ compound lies outside the $\frac{3}{2}\frac{3}{2}$ isobar peak (130 events); *b*) inside the peak (160 events).

Thus we are led to conclude that the contribution of the diagram of Fig. 26 *a*) cannot be isolated, at the present energy, from more complicated interactions.

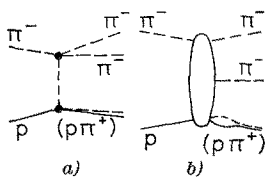

Fig. 26. – Diagrams for $(p\pi^+)$ isobar production: *a*) in the case of the OPE model; *b*) for a core interaction.

It seems however that, according to CARMONY *et al.* [12], such a separation begins to appear at an incident π^- momentum of 2.03 GeV/c.

No evidence has been obtained of the occurrence of ρ production in four-prong events. This can be understood if, as observed by ALFF *et al.* [2n] ρ's are generally produced simultaneously with the $\frac{3}{2}\frac{3}{2}$ isobar. This isobar should occur here in its neutral state and should be observed in its $(p\pi^-)$ decay. But the threshold for this reaction in the center-of-mass is around $1230+750=1980$ MeV. Since the present center-of-mass energy is only 1970 MeV, it is not surprising that the reaction is not observed. Moreover, isotopic-spin arguments unfavour the production of the $(p\pi^-)$ isobar in our experiment with regard to the $(p\pi^+)$ isobar in that of ALFF *et al.*

Figure 28 shows the $(\pi^+\pi^-)$ mass spectrum together with the phase-space prediction.

---

[12] D. D. CARMONY, F. GRARD, R. T. VAN DE WALLE and NGUYEN-HUU XUONG: *Intern. Conf. on High-Energy Physics at CERN* (1962), p. 44.

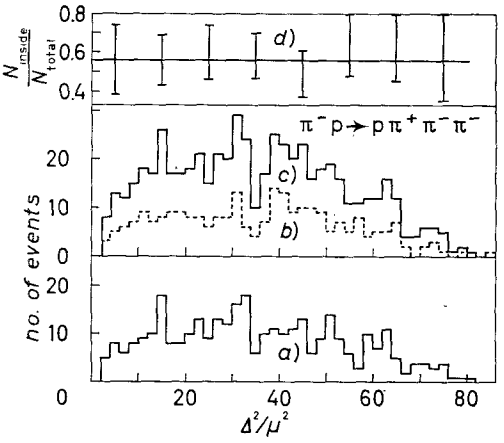

Fig. 27. – Momentum transfer distributions to the ($p\pi^+$) compound: *a*) inside the $\frac{3}{2}\frac{3}{2}$ isobar (1160 MeV$\leqslant M_{p\pi^+}\leqslant$ 1280 MeV); *b*) outside ($M_{p\pi^+}<$ 1160 MeV, $M_{p\pi^+}>$ 1280 MeV); *c*) total spectrum; *d*) ratio between the number of events inside the isobar and the total number of events, as a function of the momentum transfer.

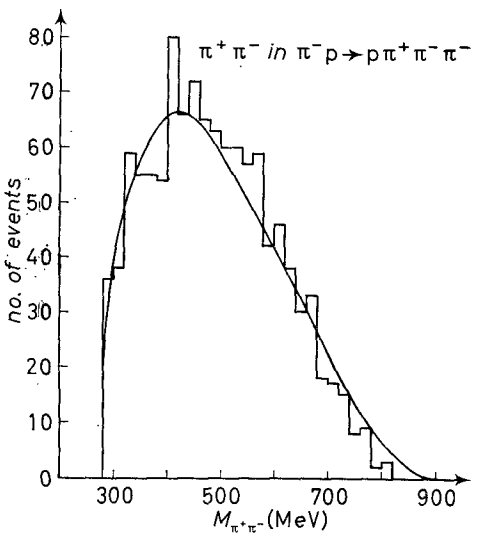

Fig. 28. – ($\pi^+\pi^-$) mass spectrum (570 events).

5·2. $p\pi^+\pi^-\pi^-\pi^0$ *events.* – For these events the most important question is to know whether they occur through an intermediate production of the ω^0 or η-mesons, subsequently decaying into three pions.

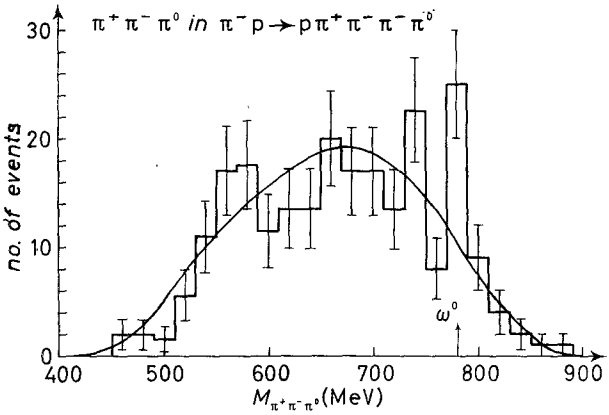

Fig. 29. – ($\pi^+\pi^-\pi^0$) mass spectrum (2×118 events).

The total number of events of this kind was 118 corresponding to a production cross-section of (0.18 ± 0.02) mb. Figure 29 shows the mass spectrum

of the neutral tripion and the corresponding expected statistical distribution. Of course, there are two points plotted on the graph per event.

No significant peak can be seen at 550 MeV, where η is expected.

The same $M_{\pi^+\pi^-\pi^0}$ spectrum exhibits a peak at (780÷790) MeV, which corresponds to the known mass of ω^0. This peak, which is located at the end of the phase-space distribution and from which it emerges by ~ 3 standard deviations, could possibly be attributed to ω^0's created in $\pi^-p \to \pi^-p\,\omega^0$ interactions. However the statistical accuracy is limited and rather large fluctuations can be expected. In fact, other peaks appear in the diagram of Fig. 29 which are certainly due to such an origin.

5·3. $n\pi^+\pi^+\pi^-\pi^-$ *events.* – 74 events of this type have been measured corresponding to a production cross-section of (0.12 ± 0.01) mb. Nothing unexpected has been observed. Within the limited statistics, the mass spectrum for the compound $(\pi^+\pi^+\pi^-\pi^-)$ is quite compatible with that predicted by phase-space.

6. – Conclusion.

All considerations developed so far for events with small momentum transfers $(1.5 \leqslant \Delta^2/\mu^2 < 8)$ point to an agreement with the validity of the OPE mechanism as a largely dominant process, at least when the mass of the dipion is in the vicinity of the ρ mass. The Treiman-Yang test seems to suggest that some other mechanism has to be taken into account for processes producing a dipion with a mass outside the resonance region.

Concerning events with large Δ^2, little can be said with confidence, apart from the fact that the OPE model becomes a less satisfactory approximation. When one tries to be more precise and extract quantitative results from the experimental data, difficulties arising from statistical uncertainties and from the lack of a definite model become rapidly prohibitive.

* * *

We gratefully acknowledge the assistance of MM. R. LEVY-MANDEL and P. LEFRÈRE and their staffs for their efficient operation of Saturne and of the external beam facilities during the course of this experiment. The 50 cm liquid hydrogen bubble chamber was constructed and operated by Mr. P. PRUGNE and his crew; our endeavour was greatly eased by their excellent service. Further great contributions were made by Mr. B. TSAI and his co-workers to all problems relative to the magnetic coils of the L.H.B.C. and to the beam magnets.

We are very indebted to MM. A. AMOUYAL and F. MENGIN of the Service de Calcul Electronique who kindly assisted us in our tedious data-processing on the Saclay IBM 7090. Our thanks also to the staff of the Centro di Cal-

colo del CNEN, Bologna (IBM 704). The Berkeley and CERN programs (GUTS and GAP) were used for this work, and we are greatly indebted to our colleagues at these laboratories for their kindness in giving us the programs.

Many illuminating and informative discussions were held with MM. F. SELLERI, M. JACOB and A. STANGHELLINI.

Finally, thanks go to all of the technicians and scanners of our groups, who, by untiring efforts, have ensured the proper functioning of the experiment and the most efficient scanning and measurements of the film.

RIASSUNTO (*)

Si riferisce sullo studio delle interazioni nelle collisioni π^-p ad un impulso dei pioni di 1.59 GeV/c, eseguito con la camera a bolle ad idrogeno liquido da 50 cm di Saclay, funzionante in un campo magnetico di 17.5 kG. I risultati ottenuti riguardano essenzialmente lo scattering elastico e quello anelastico accompagnati dalla produzione o di un solo pione nelle interazioni $\pi^-p \to p\pi^-\pi^0$ o $n\pi^-\pi^+$, o di più di un pione negli eventi a quattro rami. La distribuzione angolare osservata nello scattering elastico entro la regione di diffrazione, può essere approssimata con una legge esponenziale. Dal valore estrapolato per lo scattering in avanti, così ottenuto, si ha $\sigma_{el} = (9.65 \pm 0.30)$ mb. Nel caso della produzione di un solo pione si dànno gli spettri di massa effettivi dei dipioni $\pi^-\pi^0$ e $\pi^-\pi^+$. Ciascuno di essi presenta la corrispondente risonanza ρ^- o ρ^0 nella regione di $\sim 29\mu^2$ (μ=massa del pione carico). I picchi ρ sono particolarmente conspicui negli eventi con basso impulso trasferito (Δ^2). La distribuzione dei ρ^0 presenta un picco secondario a $\sim 31\mu^2$ dovuto probabilmente al processo $\omega^0 \to \pi^-\pi^+$. Si valuta che il rapporto di suddivisione $(\omega^0 \to \pi^+\pi^-)/(\omega^0 \to \pi^+\pi^-\pi^0)$ sia circa il 7%. Si interpretano abbastanza bene questi risultati nello schema delle interazioni periferiche secondo il modello con scambio di un pione (OPE), sino a valori di $\Delta^2/\mu^2 \sim 10$. In particolare il rapporto ρ^-/ρ^0 è dell'ordine di 0.5, come quel modello predice. Inoltre la distribuzione dell'angolo di Treiman-Yang è compatibile con una distribuzione isotropica all'interno del picco ρ. La distribuzione di $\sigma_{\pi^+\pi^-}$, calcolata con l'uso della formula di Chew-Low che si suppone valida nella regione fisica di Δ^2, dà un massimo sensibilmente più basso del valore $12\pi\lambda^2 = 120$ mb che ci si attende per uno scattering elastico $\pi\pi$ in risonanza nello stato $J=1$ al picco del ρ. Però un fattore di correzione alla formula di Chew-Low, introdotto da SELLERI, dà un accordo abbastanza buono con il valore previsto. Un'altra distribuzione, cioè la distribuzione di Δ^2, almeno per $\Delta^2 < 10\mu^2$, concorda abbastanza bene con il carattere periferico dell'interazione che cointeressa la risonanza ρ. Le distribuzioni angolari del π^- nel sistema di quiete del ρ presentano un comportamento diverso per il ρ^- e per il ρ^0. Mentre la prima è simmetrica, come riferito in un lavoro precedente, l'ultima presenta una chiara asimmetria dei π^- in avanti. Le principali caratteristiche dei risultati degli eventi a quattro rami sono: 1) il verificarsi dell'isobaro $(p\pi^+)_{\frac{3}{2}\frac{3}{2}}$ negli eventi $\pi^-p \to \pi^+\pi^-\pi^-$ e 2) la possibile produzione della risonanza $\omega^0 \to \pi^+\pi^-\pi^0$ negli eventi $\pi^-p \to p\pi^-\pi^+\pi^0$. Non si sono osservati ρ negli eventi a quattro rami.

(*) *Traduzione a cura della Redazione.*